Sumana et al., J Theor Comput Sci 2015, 2:2
DOI:10.4172/2376-130X.1000126

Journal of
Theoretical & Computational Science

Research Article Open Access

Investigation of the Effect of Fiber Orientation on FML Hollow Shaft Subjected to Static Torsion Loading

Sumana BG[1]*, Vidya Sagar HN[1], Krishna M[2]

[1]*Department of Mechanical Engineering, MRS University, Visvesvaraya college of Engineering, KR Circle, Bangaolre, Karnataka 560001, India*
[2]*Department of Mechanical Engineering, RVCE, KR Circle, Bangaolre, Karnataka 560001, India.*

Abstract

In this study, the torsional behavior of cylindrical FML hollow shafts was examined by a combined experimental and numerical approach. The FML hollow shafts with glass fibers wound on Al metallic liner at different fiber orientations were prepared using filament winding machine. To examine the effect of fiber orientation, FML hollow shafts of 0/90°, 60/30°, ± 45° and ± 55° fiber orientations were considered. Three different FRP thicknesses of 1, 2 and 3 mm were selected for all fiber orientations to study the torsional buckling and deformation behaviour of FML hollow shafts. Numerical investigation using ANSYS static and linear analysis was performed to validate the end and transition effects of torsional phenomenon. Both the experimental and numerical results showed FML hollow shafts with 0/90° fiber orientation possessed higher torsional strength as compared to FML hollow shafts with 60/30°, ± 45° and ± 55° fiber orientation.

Keywords: Fml hollow shaft; Fiber orientation; Frp thickness; Torsion; Buckling; Ansys

Introduction

Hollow shafts used to transmit power find its application in automotives, aerospace, cooling towers etc. Though most of drive shafts were manufactured from monolithic high-strength alloys [1], they possessed low power transmission efficiency due to their weight inertia [2]. With this regard, researchers worked on lighter and strong shaft materials to improve the efficiency of power transmission [3]. Advanced polymer composite materials appear extremely attractive due to their high strength-to-weight and high stiffness-to-weight ratios [4]. The polymer composite shafts enhance the efficiency of power transmission, but their mechanical properties degrade due to creep and fatigue loads during service [5]. To improve creep and fatigue resistance of the polymer composites under torsional conditions co-cured composite shafts were investigated [6].

At the same time, local and general instability arising from the action of torsional loads often limited the loading capacity of composite shafts which limits their applications in power transmission [7]. Further fiber reinforced polymer (FRP) laminated hollow shafts exhibit significant buckling sensitivity to geometric shape imperfections, thickness variations and local ply-gaps [4] which lead to structural instability resulting in shear buckling. Stiffened cylinders such as filament wound tubes and fiber metal laminate (FML) cylinders were preferred due to their high energy absorption ability [8]. Thus, a combination of lightweight composite materials and stiffened structure efficiently enhances the load carrying capability and increases the shear buckling strength [9]. These composite shafts referred to as hybrid shafts or FML hollow shafts by some of the researchers eliminates the use of two-piece shafts [10], thus reducing the weight and increasing the efficiency of the structure.

In this context, researchers developed hybrid shafts made of aluminum-carbon epoxy composites [10], steel-carbon epoxy composites [11], carbon-glass epoxy composites [8,12] etc., for optimizing the process parameters such as fiber orientation, FRP thickness, stacking sequence and number of layers. They found that the fiber orientation, stacking sequence and number of layers significantly influence the shear buckling behavior of hybrid composite shafts [13].

An efficient design of FML hollow shaft could be achieved by selecting a suitable combination of the above mentioned parameters, which are specified to minimize the chance of failure and to meet the performance requirements. This motivated the study of torsional buckling of FML hollow shafts made of Al-glass-epoxy composites by experimental and numerical approach. The objective of the work is to optimize the fiber orientation and FRP thickness for shear buckling behavior of FML hollow shaft.

Experimental Studies

The FML hollow shaft was a cylinder with aluminum (Al) metallic liner of inner diameter 40 mm, 1 mm thickness and 300 mm length on which glass fibers reinforced with epoxy resin was wound at different orientations and thicknesses. Using filament winding machine, a total of twelve (three specimens of each orientation) FML hollow shafts were prepared with fibers wound at 0/90°, 60/30°, ± 45° and ± 55° orientations and thickness of FRP maintained at 1, 2 and 2.5 mm. The cured FML hollow shafts were subjected to torsional loading using a torsion testing machine which is as shown in Figure 1. The lengths of constraint region and the loading region were 25 mm and 30 mm respectively. The torsion testing machine can apply torque up to a maximum of 60 Nm. The torque applied on the FML hollow shafts was increased in steps of 2.5 Nm with a static loading rate of 1 Nm per second till failure occurred due to shear torsional buckling. The mechanical properties of Al 6061 [14] and glass-epoxy composite material [15] are listed in Table 1.

Numerical Solution

A numerical 3D-FE model was developed to replicate the experimental tests as well as to identify the main factors influencing shear buckling. Simulation has been carried out by using ANSYS 14.5 finite element package.

***Corresponding author:** Sumana BG, Research Scholar, Department of Mechanical Engineering, University Visvesvaraya college of Engineering, K R Circle, Bangaolre, Karnataka 560001, India, Tel: +91 9945490498;Fax: +91 9945490498; E-mail: sumogh76.gec@gmail.com

Received April 28, 2015; **Accepted** May 23, 2015; **Published** May 30, 2015

Citation: Sumana BG, Vidya Sagar HN, Krishna M (2015) Investigation of the Effect of Fiber Orientation on FML Hollow Shaft Subjected to Static Torsion Loading. J Theor Comput Sci 2: 126. doi:10.4172/2376-130X.1000126

Citation: Sumana BG, Vidya Sagar HN, Krishna M (2015) Investigation of the Effect of Fiber Orientation on FML Hollow Shaft Subjected to Static Torsion Loading. J Theor Comput Sci 2: 126. doi:10.4172/2376-130X.1000126

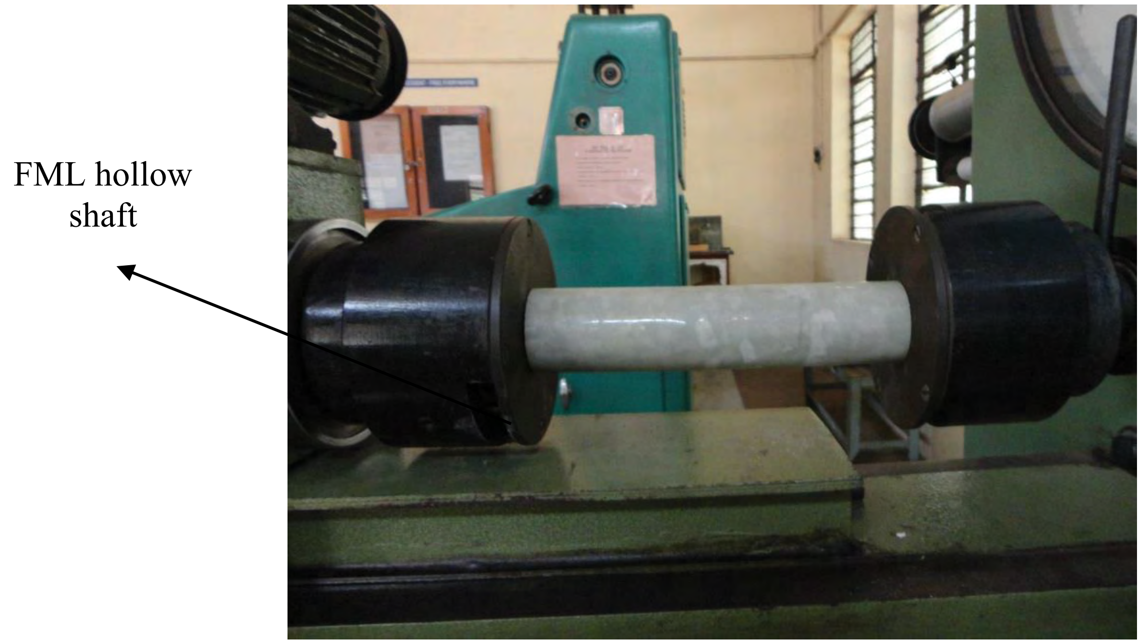

Figure 1: Torsion testing machine with FML shaft.

A detailed description of the steps involved in using the software for analysis of FML hollow shafts is described in the following section.

Element type and material properties

The element type used was SHELL281 for both Al metallic liner and FRP. SHELL281 is suitable for analyzing moderately-thick shell structures. It has eight nodes with six degrees of freedom at each node: translations in the x, y, and z axes, and rotations about the x, y, and z-axes. This element may be used for layered applications for modeling composite shell structures. The mechanical properties needed are modulus of elasticity (E) and Poisson's ratio (υ) for linear isotropic material i.e., aluminum and orthotropic properties for FRP.

Modeling and meshing

Al metallic liner of 1 mm thickness is input as one layer, on which FRP of 0.25 mm thickness with respective winding angle is considered for the finite element analysis. The layer stacking sequence of 2 mm FRP wound on 1 mm Al metallic liner is shown schematically in Figure 2(a). A hollow cylinder was created using the option of solid cylinder and then deleting the volume and areas. This was done in order to maintain same displacement of the interface. Based on the convergence test the composite cylinder was meshed free as shown in Figure 2(b) with a maximum of 3145 nodes.

Aluminum	Value
Young's Modulus	70 GPa
Poisson's ratio	0.33
Specific density	2.7 g/cc
Glass/Epoxy composite	Value
E_1	53.48 GPa
E_2, E_3	17.7 GPa
$υ_{12}$	0.278
$υ_{23}$	0.4
$υ_{13}$	0.278
G_{12}, G_{23}	5.83
G_{13}	5.78
Density	2.1 g/cc

Table 1: Material properties of Aluminum (Al 6061-T6) and glass/epoxy composite.

Constraints and loading

On one end of the FML hollow shaft a length of 25 mm was constrained along all degrees of freedom, as shown in Figure 2(c). On the other end of the FML hollow shaft along a length of 30 mm (similar to the grips used in experimental tests) a torque of M=1 Nm was applied about Z-axis as shown in Figure 2(d). The torsional load was increased in steps of 1 Nm per second till the shaft buckled. The traditional approach to hollow shaft design was to predict the buckling load using a linear bifurcation buckling analysis with the nominal structural dimensions and material properties of an idealized geometrically perfect shell [4]. Static analysis and Eigen buckling analysis using Block Lanczos extraction method were performed in sequence to obtain the critical buckling torque. Static buckling was performed to determine the pre-buckling deformation. The linear eigenvalue buckling analysis was used to determine buckling load – initial/critical load at which a structure becomes unstable and buckled mode shapes - the characteristic shape associated with a structure's buckled response [16]. It only predicts the pre-buckling deformation, but does not solve the magnitude of deformation post buckling [17]. The results for all the FML hollow shafts with their respective orientation and thickness are discussed in the following section.

Results and Discussion

Effect of fiber orientation and FRP thickness on torque – experimental analysis

The experimental results of the FML hollow shaft subjected to torsional load were as plotted in Figure 3. The y-axis represent load while x-axis indicate relative angle of rotation with one end constrained

Citation: Sumana BG, Vidya Sagar HN, Krishna M (2015) Investigation of the Effect of Fiber Orientation on FML Hollow Shaft Subjected to Static Torsion Loading. J Theor Comput Sci 2: 126. doi:10.4172/2376-130X.1000126

and torsional load applied at the other end. It was observed that the ultimate strengths of the repeated hollow shafts were similar. The FML hollow shafts buckle when they lost their stability, and the circular cross-section becomes ovoid. Based on the observations during the experimentation process and analysis of test data, the FML hollow shafts were considered to experience three stages under loading until failure. In the first stage, load applied on the shaft was absorbed by both the Al metallic liner and FRP, indicating elastic behavior of the metallic liner. Minor cracks occurred in the tension zone of FRP layer with increase in load. With propagation of crack, the FRP under tension gradually lost its strength. In the second stage, FRP in the tension zone completely lost its strength while the FRP in compression continue to resist the load. At the end of second stage, the Al metallic liner reaches yielding. In the third stage, the FRP in compression completely lost its strength and large deformation occurred in the compression zone of Al metallic liner. The outer FRP layers were taken out from the failed hollow shafts for observation of crack pattern. The angle between the crack and axis along the length of FML hollow shaft was approximately 40°.

Thickness of FRP influences the buckling behavior of FML hollow shaft. It was observed that for a FML hollow shaft of FRP thickness 1 mm, both the Al metallic liner and FRP failed simultaneously. Torsional buckling occurred at around 10°–15° angle of twist and torque reduced drastically once the FML hollow shaft experienced buckling. In FML hollow shafts of FRP thicknesses 2 and 2.5 mm, torsional buckling occurred beyond 15° angle of twist and cracking of FRP in different layers was observed before failure of the shaft.

Effect of fiber orientation and FRP thickness on torque – numerical analysis

A linear eigenvalue buckling analysis estimates the maximum torque that can be supported prior to losing stability [16]. The numerical results of pre-buckling shear deformation of FML hollow shafts with 0/90°, 60/30°, ± 45° and ± 55° fiber orientations and thickness of FRP 1, 2 and 2.5 mm are as shown in Figure 4. The typical snap shots of torsional pre-buckling modes of FML hollow shafts are as shown in Figure 5. All the considered FML hollow shafts increase linearly up to shear buckling point. Though the shaft material was heterogeneous, torque was proportional to angle of twist similar to the behavior of isotropic material. This shows the linear behavior of Al metallic liner along with glass fibers reinforced with epoxy. It was observed that irrespective of FRP thickness FML hollow shaft of 0/90° fiber orientation exhibit maximum buckling strength. This was due to the fact that fibers oriented along 0° increase the axial strength and fibers oriented in 90° increase hoop strength thereby increasing the shear buckling strength [18] of the shaft.

For 10° angle of twist, the torque exhibited by FML hollow shaft of 0/90° fiber orientation with FRP thickness 1, 2 and 2.5 mm was 6.54, 9 and 10 Nm respectively. This indicates that torsional strength increased with increase in FRP thickness up to 2.5 mm.

In FML hollow shafts of 3 mm FRP thickness premature buckling occurred due to fiber pull-out and slipping of fibers in the outer layer. Also, the numerical analysis issued warnings stating the required radius-to-thickness ratio should be greater than 5. Extrapolation to a higher number of layers gives in general inaccurate results [19].

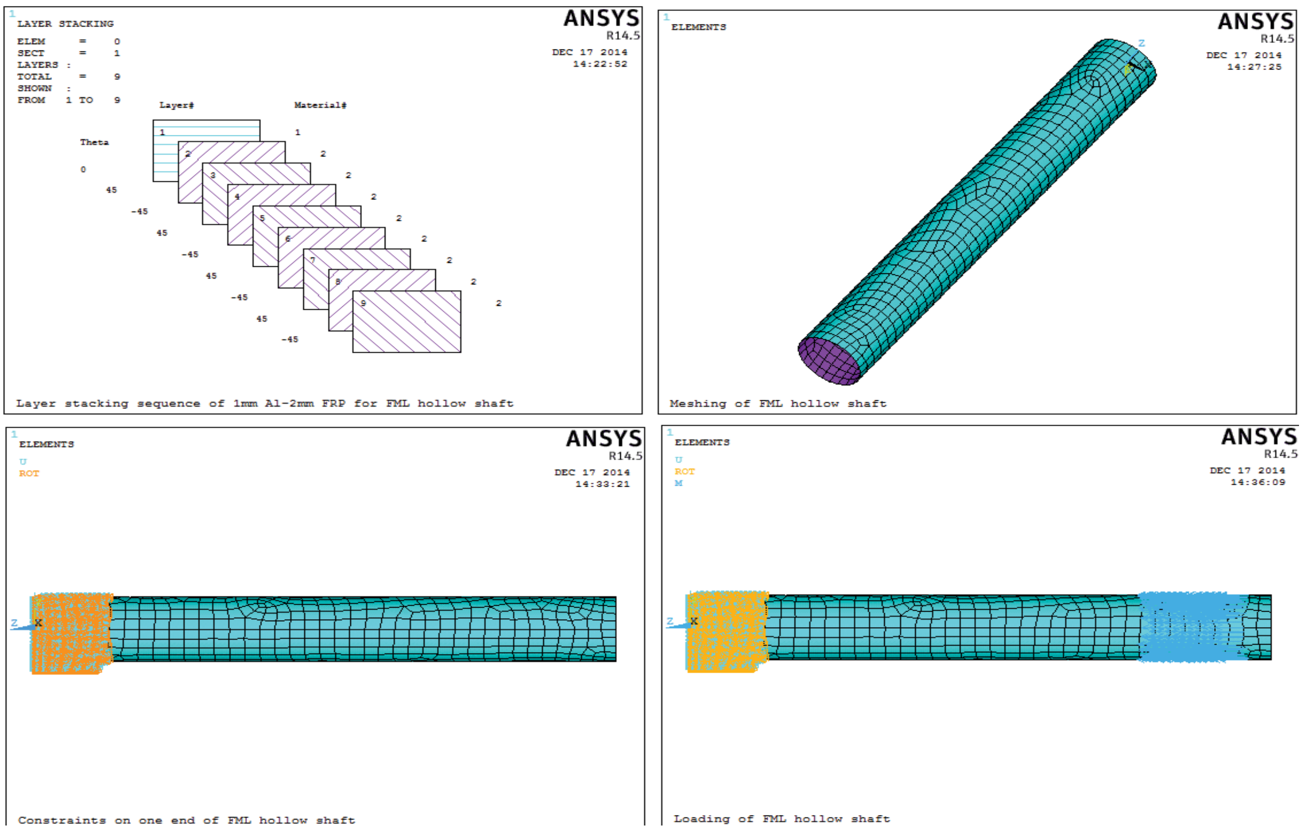

Figure 2: FEA model of (a) Layer stacking sequence, (b) Meshing, (c) Constraining and (d) Loading of FML hollow shaft.

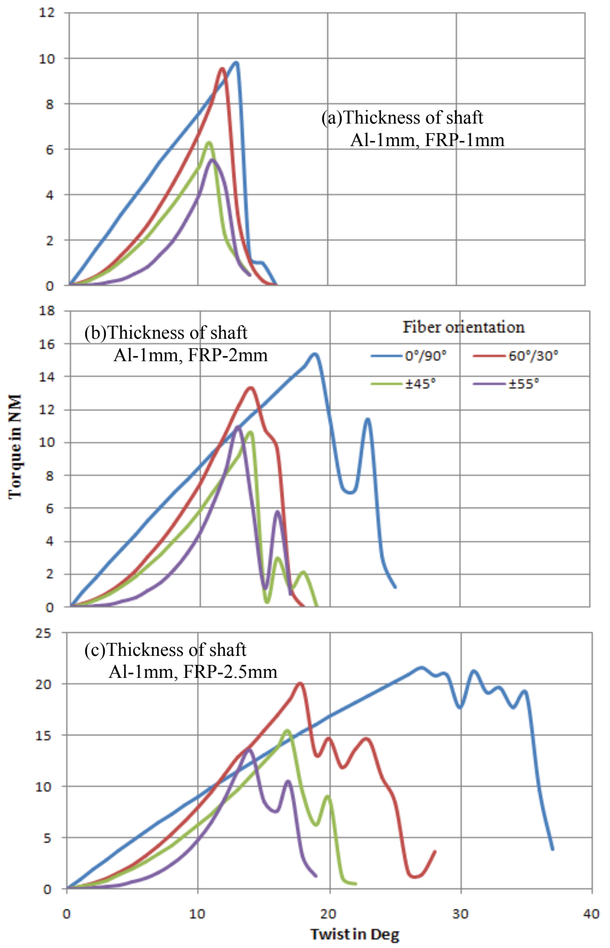

Figure 3: Effect of fiber orientation and twisting angle on torsional strength of FML hollow shafts - by experiment.

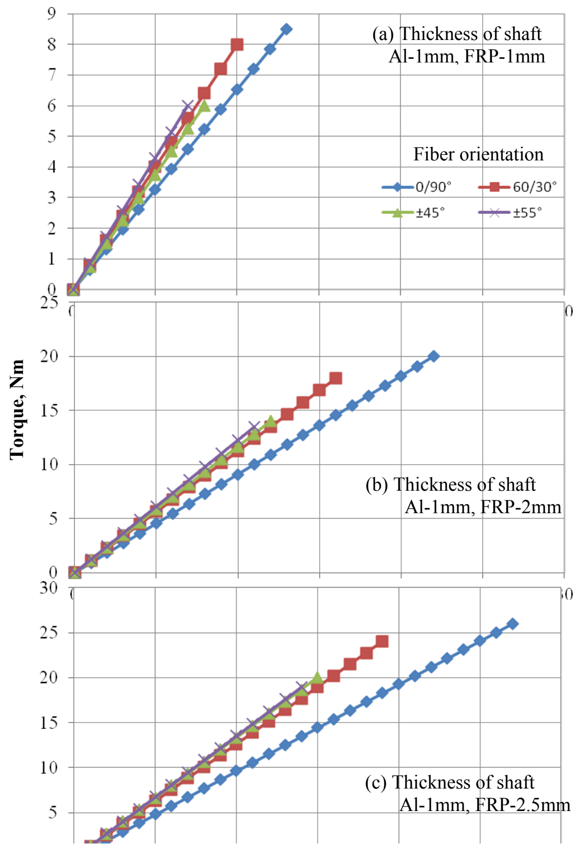

Figure 4: Effect of fiber orientation and twisting angle on torsional strength of FML hollow shafts - By FEA.

Similarly, at 5° angle of twist irrespective of FRP thickness, the value of torque increased for FML hollow shafts of 60/30°, ± 45° and ± 55° fiber orientation. This was attributed to the shear nature of fibers resulting in low strain-to-failure. The ductility of FML hollow shaft can be enhanced by increasing the thickness of FRP [20] or by choosing the fiber orientation that has a higher strain-to-failure [21]. On the other hand, the angle of ± 45° fiber orientation was used to obtain the maximum shear strength [18].

Increasing the thickness of FRP or number of layers increases the static torque capacities and angle of twist of FML hollow shafts as shown in Figure 6. The critical load is lower for a thinner shell and this buckling phenomenon agrees well with experiments which got the conclusion that the bifurcation torque and the stability losing torque increase with increasing shell thickness [22]. It was observed that as the thickness of FRP increased, the buckling torque increased exponentially due to increasing shear strength of the laminate due to increasing fiber modulus [12] as shown in Figure 6. The stiffness and strength of laminated glass fibers depend upon shear coupling between the glass plies through the polymer. The polymeric interlayers provide shear stresses that constrain the relative sliding of the glass fiber plies [19]. Similar behavior was observed in researches performed by [4,12,20].

Figure 7 shows typical buckling modes of FML hollow shafts subjected to static torsion loading.

Comparison of experimental and numerical results

The numerical results of the effect of FRP thickness on buckling torque due to fiber orientation of FML hollow shaft were compared with the experimental results as shown in Table 2. The difference of buckling torque ranged from 3% to 29% for FML hollow shafts of FRP thickness 1, 2 and 2.5 mm. The average deviation was 6.5, 23.5 and 21.8 for FML hollow shafts of FRP thickness 1, 2 and 2.5 mm respectively. These differences occur because in finite element analysis it is assumed that the FML hollow shaft is homogenous in terms of dimensions, material properties, fiber layers and winding pattern. While, through the experimental test homogeneity is never exactly the same throughout the positions in each FML shaft [20].

In FML hollow shafts of FRP thickness 1 mm, the experimental values were greater than FEA values. This indicates the material property of Al metallic liner dominating the structure and hence the shaft behavior is homogeneous. But, in FML hollow shafts of FRP thickness 2 and 2.5 mm, the FEA values were greater than experimental values. The shaft behavior was heterogeneous due to the dominating material property of FRP. The Finite element model have no imperfection or any defect, hence the accumulation of shear stress in a band form explains the location where the buckling occurs or the location at the cross-section that was more susceptible to deflection due to a reduced

Citation: Sumana BG, Vidya Sagar HN, Krishna M (2015) Investigation of the Effect of Fiber Orientation on FML Hollow Shaft Subjected to Static Torsion Loading. J Theor Comput Sci 2: 126. doi:10.4172/2376-130X.1000126

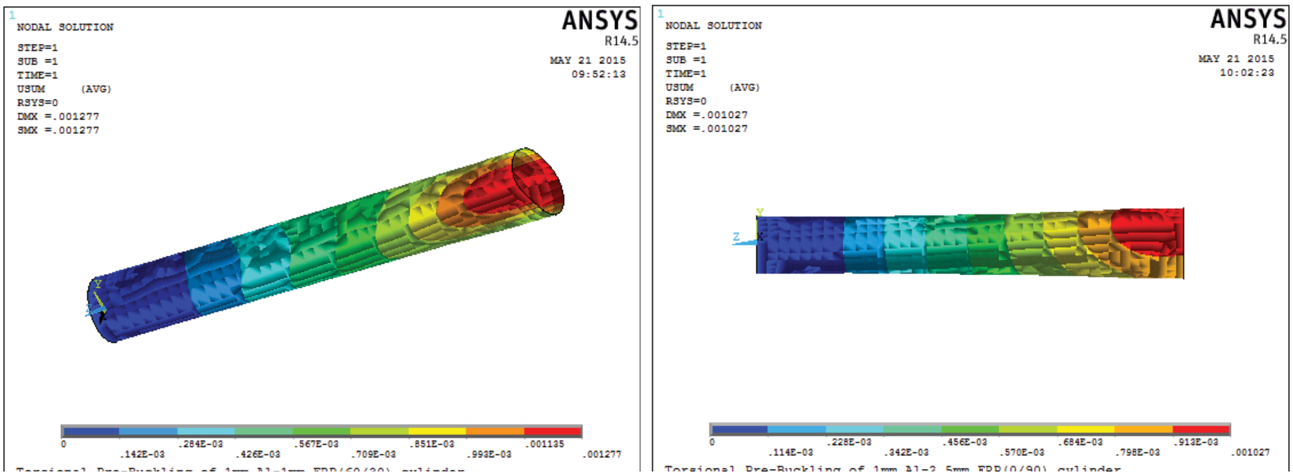

Figure 5: Typical Pre-buckling modes of FML hollow shafts under static torsion loading.

	1 mm			2 mm			2.5 mm		
	Expt	FEA	% Deviation	Expt	FEA	% Deviation	Expt	FEA	% Deviation
0/90°	9.69	8.5	14	15.27	20	23.65	21.55	26	17.13
60/30°	9.39	8	17.38	13.31	18	26.08	19.82	24	17.43
± 45°	6.17	6	2.83	10.46	14	25.28	15.26	20	23.68
± 55°	5.52	6	8	10.93	13.5	19.03	13,43	19	29.28

Table 2: Comparison of experimental and numerical values of buckling torque (Nm) for different FRP thicknesses.

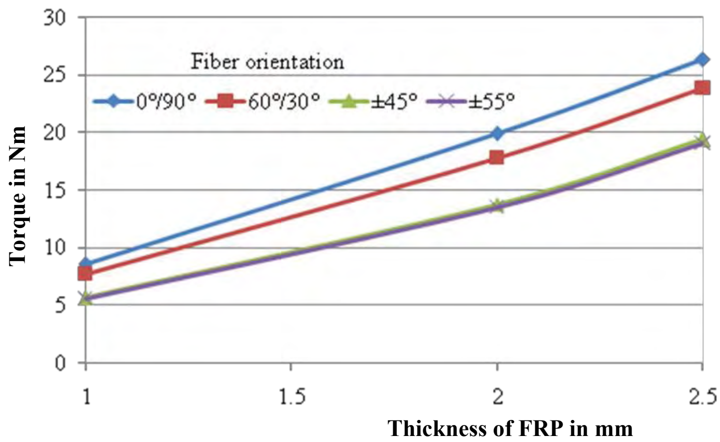

Figure 6: Effect of FRP thickness on torsional strength of FML hollow shafts.

bending stiffness along the hoop direction [12].

Conclusion

Effect of fiber orientation and FRP thickness on the torsional buckling of FML hollow shafts was investigated experimentally and numerically. Based on this study, the following conclusions can be drawn:

- FML hollow shaft with 0/90° fiber orientation exhibit maximum buckling torque due to higher hoop strength.
- Buckling torque reduced as the orientation of fiber reduced from 90° to 0°, irrespective of FRP thickness.
- In FML hollow shaft of 1 mm FRP thickness, the Al metallic liner and FRP fail simultaneously without prior fiber failure.
- Breaking of fibers and cracks in FRP occur as the thickness

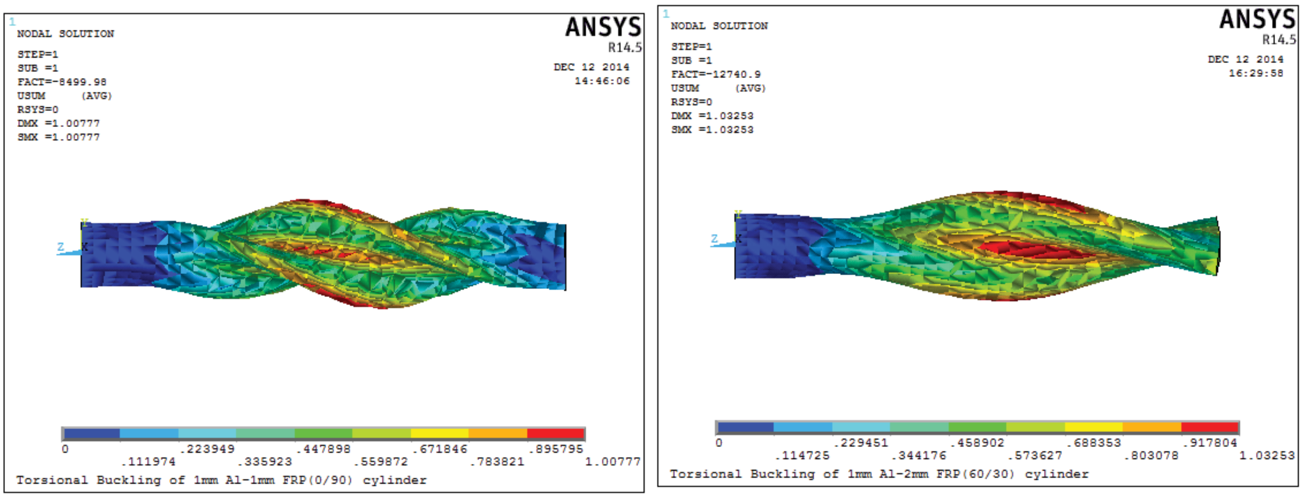

Figure 7: Torsional buckling modes of FML hollow shafts.

of FRP increases.

- The behavior of FML hollow shaft of 1 mm FRP thickness was homogeneous while FML hollow shafts of 2 and 2.5 mm FRP thickness was heterogeneous.
- The buckling torque and angle of twist increased with increase in FRP thickness.
- In numerical analysis, all the considered FML hollow shafts show a linear behavior until shear buckling load is reached.
- The experimental and FE results exhibited sufficient agreement in comparisons of torque-angle of twist relations.

References

1. Salzar RS (1999) Design considerations for rotating laminated metal-matrix-composite shafts. Composites Science and Technology 59: 883-896.
2. Sevkat E, Tumer H (2013) Residual torsional properties of composite shafts subjected to impact loadings. Materials and Design 51: 956-967.
3. Stuart HL (1984) Design of power transmitting shafts. NASA Reference publication 1123, Lewis Research, Center Cleveland, Ohio, pp 20-21.
4. Bisagni C, Cordisco P (2003) An experimental investigation into the buckling and post-buckling of CFRP shells under combined axial and torsion loading. Composite Structures 60: 391-402.
5. Bhaumik SK, Rangaraju R, Parameswara MA, Venkataswamy MA, Bhaskaran TA, et al. (2002) Fatigue failure of a hollow power transmission shaft. Engineering Failure Analysis 9: 457-467.
6. Cho DH (1998) Manufacturing of Co-Cured Composite Aluminum Shafts with Compression during Co-Curing Operation to Reduce Residual Thermal Stresses. Journal of Composite Materials 32: 1221-1241.
7. Shokrieh MM, Hasani A, Lessard LB (2004) Shear buckling of a composite drive shaft under torsion. Composite Structures 64: 63-69.
8. Sevkat E, Tumer H, Kelestemur MH, Dogan S (2014) Effect of torsional strain-rate and lay-up sequences on the performance of hybrid composite shafts. Materials and Design 60: 310-319.
9. Huang L, Sheikh AH, Ching-Tai N, Griffith MC (2014) an efficient finite element model for buckling analysis of grid stiffened laminated composite plates. Composite Structures 122: 41-50.
10. Lee DG, Kim HS, Kim JW, Kim JK (2004) Design and manufacture of an automotive hybrid aluminum/composite drive shaft. Composite Structures 63: 87-99.
11. Kim HS, Kim BC, Lim TS, Lee DG (2004) Foreign objects impact damage characteristics of aluminum / composite hybrid drive shaft. Compos Struct 66: 377-389.
12. Badie MA, Mahdi E, Hamouda AMS (2011) an investigation into hybrid carbon/glass fiber reinforced epoxy composite automotive drive shaft. Materials and Design 32:1485-1500.
13. Swanson SR (1997) Introduction to design and analysis with advanced composite materials. Upper Saddle River, Prentice Hall, New Jersey, USA.
14. James MG (2004) Mechanics of materials (6thedn.) Thomson Brooks/Cole, p. 913.
15. Soden PD, Hinton MJ, Kaddour AS (2004) Lamina properties, lay-up configurations and loading conditions for a range of fibre reinforced composite laminates. Failure criteria in fiber reinforced polymer composites: the world-wide failure exercise.
16. Wang X, Xiao J, Zhang YC (2004) A method for solving the buckling problem of a thin-walled shell. International Journal of Pressure Vessels and Piping 81: 907-912.
17. Wai-Fah C, Atsuta T (2008) Theory of beams and columns. In: Plane behaviour and design.
18. Talib ARA, Ali A, Badie MA, NAC Lah, Golestaneh AF (2010) Developing a hybrid, carbon/glass fiber-reinforced, epoxy composite automotive drive shaft. Materials and Design 31: 514-521.
19. L Galuppi, G Royer-Carfagni (2014) Enhanced Effective Thickness of multi-layered laminated glass. Composites: Part B 64: 202-213.
20. Mutasher SA (2009) Prediction of the torsional strength of the hybrid aluminum/composite drive shaft. Materials and Design 30: 215-220.
21. Callens MG, Gorbatikh L, Verpoest I (2014) Ductile steel fibre composites with brittle and ductile matrices. Composites: Part A 61: 235-244.
22. Xu X, Ma J, Lim CW, Ge Z (2010) Dynamic torsional buckling of cylindrical shells. Computers and Structures 88: 322-330.